Catena 254 (2025) 108967

Contents lists available at ScienceDirect

Catena

journal homepage: www.elsevier.com/locate/catena

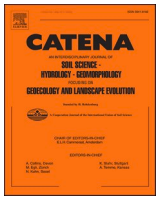

Rapid and significant lithium isotope response to afforestation in Icelandic topsoils

Xianyi Liu [a,b,*], David J. Wilson [a], Kevin W. Burton [c], Bjarni Diðrik Sigurdsson [d], Julia C. Bos [d], Wesley T. Fraser [e], Philip A.E. Pogge von Strandmann [a,f,*]

[a] LOGIC, Department of Earth Sciences, University College London, London WC1E 6BT, UK
[b] Department of Earth Science, Utrecht University, 3584CB, the Netherlands
[c] Department of Earth Science, Durham University, Durham DH1 3LE, UK
[d] Faculty of Environmental and Forest Sciences, Agricultural University of Iceland, H66H+9R9, Hvanneyrabraut, 311 Hvanneyri, Iceland
[e] Geography, Department of Social Sciences, Oxford Brookes University, Oxford OX3 0BP, UK
[f] MIGHTY, Institute of Geosciences, Johannes Gutenberg University, Mainz 55122, Germany

ARTICLE INFO

Dataset link: Data for Rapid and significant lithium isotope response to afforestation in Icelandic topsoils (Original data)

Keywords:
Silicate weathering
Lithium isotopes
Vascular plants
Soil chronosequences
Sequential leaching

ABSTRACT

Silicate weathering plays an important role in pedogenesis and the carbon cycle. Lithium (Li) isotopes are an effective tracer for the silicate weathering intensity and have been employed extensively to quantify both modern and past silicate weathering processes. The presence of vascular plants is believed to significantly influence weathering processes and pedogenesis, but how exactly plants and their ecosystems influence the behaviour of silicate weathering and Li isotopes in soils is poorly constrained. Here, we explored this question by measuring plant organs and sequentially leached fractions from soil chronosequences in Iceland spanning 25–63 years following afforestation. We found that Li isotopes were significantly fractionated within the plants during Li transport from the roots towards the leaves, and propose that ^{6}Li preferentially crosses vacuole membranes in cells, while ^{7}Li is enriched in the vascular system and accumulates in the leaves. This intra-plant fractionation could be most pronounced during plant growth when plants are subject to an excess nutrient supply. The Li isotope compositions in the exchangeable, carbonate, and oxide minerals of the afforested soils were ~ 10 ‰ higher than in those of the heathland soils, and such differences can be attributed to both the input of heavy Li isotopes from litterfall decomposition and the effect of afforestation-mediated secondary mineral formation. Overall, this study suggests that silicate weathering processes traced by Li isotopes can respond significantly and rapidly (<25 years) to forest establishment, with important implications for paleoenvironmental reconstructions and the evolution of the critical zone.

1. Introduction

Silicate weathering plays an important role in pedogenesis by dissolving primary minerals and producing secondary minerals. It also supplies alkalinity to the ocean, helping to remove CO_2 from the atmosphere and significantly influencing global climate (Walker et al., 1981). The use of plants to mediate pedogenesis and increase silicate weathering efficiency has recently been proposed to speed up this process and combat the increasingly urgent atmospheric CO_2 problem (e.g., Campbell et al., 2022; Edwards et al., 2017; Kantola et al., 2017). Conceptually, plants would acquire nutrients from substrates (i.e., rocks) and significantly influence silicate weathering in multiple direct and/or indirect ways (e.g., Dakora and Phillips, 2002; Kulmatiski et al., 2008; Lucas, 2001; Uhlig et al., 2017). The roots of plants not only mechanically break up rocks and increase relative surface areas (i.e., increase erosion and weathering rates), but also elevate soil CO_2 and organic acid levels, further enhancing chemical weathering processes (Berner et al., 2003; Jones, 1998; Rosenstock et al., 2019). However, plants also bind and stabilise soils, which can reduce erosion and limit the supply of fresh rocks, thereby reducing chemical weathering fluxes (Dontsova et al., 2020; West et al., 2005). Thus, due to a limited understanding of the dominant mechanisms of plant-mediated silicate weathering in soils, the overall efficacy of the 'weathering-enhancing mechanisms' is poorly constrained. Such complex and counteracting processes together produce diverging results for the role plants can play in weathering and pedogenesis processes over different timescales. For

* Corresponding authors at: Department of Earth Science, Utrecht University, 3584CB, the Netherlands.

https://doi.org/10.1016/j.catena.2025.108967
Received 20 November 2024; Received in revised form 23 January 2025; Accepted 17 March 2025
Available online 25 March 2025

example, moss and fungi-rock interaction experiments (with a timescale of days) suggest that plants could significantly increase silicate weathering fluxes and help the formation of soil (e.g., Bonneville et al., 2011; Lenton et al., 2012), whereas studies targeting longer timescales (e.g., >100 years) suggest that plants approaching maturity can instead inhibit silicate weathering (Balogh-Brunstad et al., 2008; Oeser and von Blanckenburg, 2020). Therefore, reliable proxies and observations across timescales are needed to track plant-mediated silicate weathering processes in soils.

Lithium (Li) isotopes are a useful tool for tracing silicate weathering processes. The two stable isotopes, ^{6}Li and ^{7}Li, have a relatively large mass difference, which allows them to exhibit a large fractionation. Lithium isotopes are not significantly fractionated during primary mineral dissolution, but are highly fractionated during secondary mineral formation (Penniston-Dorland et al., 2017). In general, ^{6}Li is preferentially adsorbed onto inner-spheres on mineral surfaces and/or incorporated into secondary mineral lattices, leaving the fluid phases enriched in ^{7}Li (Pistiner and Henderson, 2003; Pogge von Strandmann et al., 2021). The fractionation varies from 0 ‰ to over 20 ‰, depending on the binding environment (Hindshaw et al., 2019). Compared to traditional approaches to investigate weathering and compositional changes of soil, including the chemical index of alteration (CIA) proxy and mineralogical analysis (e.g., X-ray diffraction), Li isotopes are more sensitive and not substantially influenced by source-rock lithology (e.g., Pogge von Strandmann et al., 2019). Such a sensitivity of Li isotopes to weathering (i.e., secondary mineral formation) makes them a powerful tracer to deconvolve the controlling mechanisms during pedogenesis (e.g., Li et al., 2020; Rudnick et al., 2004), to investigate the evolution and material transfers in soils (Cai et al., 2024; Zhang et al., 2023), and to study the response of weathering processes to both seasonal-scale hydrological controls (Wilson et al., 2021) and geological-scale (kyr to Myr) past climate change (e.g., Hathorne and James, 2006; Misra and Froelich, 2012; Pogge von Strandmann et al., 2013).

However, despite the increasing use of Li isotopes to trace weathering processes in both modern and past soils, only limited research has utilised them to understand the interaction between plants and soils (Li et al., 2020; Pogge von Strandmann et al., 2022). Furthermore, these studies only obtained soil compositional data from a fixed point in time and therefore could not assess the response of Li isotopes over decadal or longer timescales. Such effects need to be constrained in order to reliably interpret Li isotope signals in enhanced weathering, soil science, and paleoenvironmental research. In addition, from the plants side, only a handful of studies have made preliminary assessments of the behaviour of Li isotopes within plants (Cai et al., 2024; Chapela Lara et al., 2022; Clergue et al., 2015; Lemarchand et al., 2010; Li et al., 2020; Steinhoefel et al., 2021), and the number of samples analysed has been extremely limited (e.g., four measurements were reported in Lemarchand et al. (2010) and one in Chapela Lara et al. (2022)). Thus, studying the behaviour of Li isotopes in plants and soils over decadal timescales will help us not only to understand the role of plant-mediated silicate weathering in soil dynamics, but also to further the application of Li isotopes for quantifying plant-mediated enhanced weathering in soils in relation to CO_2 sequestration goals. Considering longer geological timescales, improved constraints on plant weathering and its Li isotope signature will also help in assessing the role of silicate weathering in the Earth system during periods with a changing distribution of vascular plants on land.

Here, we analysed soil and plant samples from a soil chronosequence in Iceland to investigate the behaviour of Li isotopes during afforestation. A set of spatially extensive field plots were cleared of trees at certain times in the past and then allowed to regrow, such that each area experienced different periods of tree growth (up to 63 years). This sample set allows a comprehensive examination of the behaviour of Li isotopes during plant growth, and the effects of afforestation on weathering processes over decadal to multi-decadal timescales. The plant samples indicate significant Li isotope fractionation during tree growth, while the leachable fractions of the soils were heavily influenced by weathering changes related to the process of afforestation.

2. Samples and methodology

The samples were obtained near Lagarfljót river in East Iceland, within the largest forested area in Iceland (Sigurdsson et al., 2005) (Fig. 1). This area has a mean annual temperature of 3.4 °C and annual rainfall of ~ 740 mm. The substrates are basalt rock and rhyolitic volcanic ash from the eruption of Mt Askja in 1875 (Ritter, 2007), and the frequent volcanic eruptions in Iceland have created stratified and horizontally heterogenous soils (Arnalds et al., 1995; Ritter, 2007). This area was subject to 1000 years of extensive erosion due to deforestation and grazing (Arnalds et al., 1995), before an afforestation project started with the first plot being established in 1952. The species used in this project is Siberian larch, which normally lives for more than 100 years and can reach ~ 20 m in height. The soils in this area are classified as andosols, which contain significant amounts of dissolvable glass and amorphous secondary minerals.

In this study, soils from five plots with different afforestation ages (i.e., chronosequences L1, L2, L3, L4, and L5, with afforestation ages of 25, 31, 32, 46, and 63 years, respectively) were collected (Fig. 1). In order to mitigate the possibility of biased measurements from small sample sizes, each sample used in this study is a mixture of four individual samples collected from four transects within a plot. Note that the trees from all five sites had been thinned at least once and the use of heavy machinery may have damaged the topsoil physical properties. For comparison, we also obtained soils from a nearby tree-less heathland (H). Both shallow (~10 cm depth, layer O) and deeper (~30 cm depth, layer B) topsoils from the afforested locations were sampled and the sampling method can be found in Bos (2021), while samples from ~ 20 cm (HS) and ~ 30 cm (HD) were taken from the H location. Investigating topsoils minimises the impacts from potentially more complex sub-surface hydrological conditions, allowing a focus on the influence of plants on soils. The same region was sampled in both 2002 and 2015, and here we used the soil samples collected in 2015. Basic physical properties, pH, soil organic carbon (SOC), and soil organic nitrogen (SON) are reported in Bos (2021). In addition, samples of roots, bark, grass (ground vegetation), and leaves of the trees were also collected and dried.

The plant samples were collected from one tree at each of the five sites (L1 to L5). The plant samples of the same organ from each site were first dried and mixed, in order to homogenise the plant signals. They were then ground by agate pestle and mortar, and were fully digested using concentrated HNO_3 and H_2O_2 at 130 °C for three days.

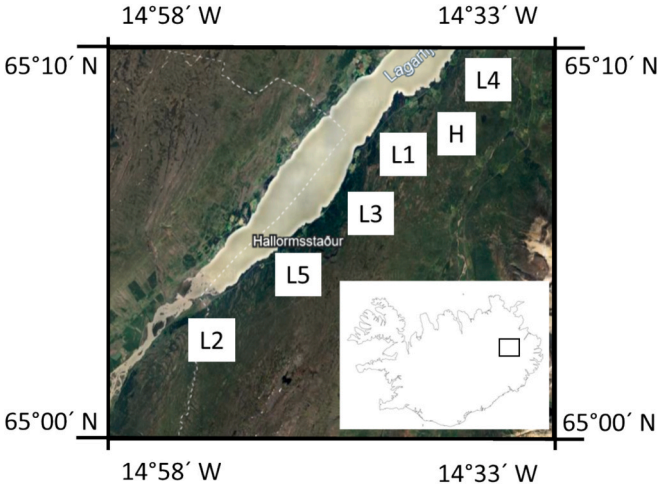

Fig. 1. Locations of the sampling sites near Lagarfljót river. H, heathland; L, larch. Modified from Ritter (2009), with image from Google Earth Pro.

The soil samples were sequentially leached to obtain the following four fractions, following previous studies (Liu et al., 2022; Pogge von Strandmann et al., 2022): 1) the exchangeable (Ex) phase (weakly-bound adsorbed cations) by adding 1 M sodium acetate and reacting at room temperature for 1 h; 2) the carbonate (Carb) phase by adding acetic acid buffered to pH 5 using 1 M sodium acetate and reacting at room temperature for 5 h; 3) the reducible (oxide, Ox) phase by adding 1 M hydroxylamine hydrochloride (HH) in 25 % acetic acid and reacting at room temperature for 1 h; and 4) the 'clay' (Cl) phase by adding 0.6 M HCl and reacting at room temperature for 1 h. The residue fractions (Rs) were then completely dissolved in a mixture of HF, $HClO_3$, and HNO_3 at 130 °C for three days. Here, the sequential leaching is conducted to obtain signals reflecting the weathering processes rather than those from primary minerals (i.e., Rs). As with all selective leaching processes, it is likely that each step is not 100 % efficient at extracting the phases of interest, and that other non-targeted phases may also be weakly attacked (Liu et al., 2022). In particular, we note that the clay leach is primarily designed to determine the Li isotope composition of this fraction, and likely does not dissolve all the clays contained in the samples (Li and Liu, 2020; Pogge von Strandmann et al., 2014). Despite potentially incomplete extraction at each step of the sequential leaching, comparing the fractions leached from similar substrates has been shown to be reasonable (Pogge von Strandmann et al., 2023). Furthermore, in basaltic weathering experiments, the combination of these leaches was able to mass balance the Li removed from solution (Pogge von Strandmann et al., 2019, 2022), which also supports the validity of this procedure. We further assess the reliability of the leaching results based on their elemental ratios in Section 4.

The extracted fractions from the sequential leaching were diluted and their elemental concentrations were measured by Varian ICP-OES and Agilent ICP-MS in the LOGIC laboratories at UCL. For the exchangeable and carbonate fractions, the samples were diluted (matrix-matched) to Na concentrations of 100 μg/ml, while the other samples were diluted to Ca concentrations of approximately 10 μg/ml. A series of standard solutions made up from single element standards (Agilent) was used for calibration. To control for potential matrix effects, the standards for the high-Na samples (i.e., exchangeable and carbonate phases) were also matrix-matched, and hence were different from those for the other samples. The analytical uncertainty (internal RSD) was better than 2 % for the ICP-OES measurements and 5 % for the ICP-MS measurements, and USGS SGR-1 and NBS 88a standards were used to assess the accuracy (which was within 5 % of the reference values).

For Li isotopes, samples containing ~ 5 ng of Li were purified via a two-stage column method with AG50W X-12 resin using 0.2 M HCl as an eluent, before being analysed on a Nu Plasma 3 MC-ICP-MS in the LOGIC laboratories at UCL (Pogge von Strandmann et al., 2019). Because Li isotopes can be highly fractionated during the ion-exchange process, we ensured that the recovery efficiency of Li was higher than 99.8 % (Gou et al., 2020). Atlantic seawater and blanks were also analysed as controls, with seawater δ^7Li values of 31.2 ± 0.2 ‰ (n = 6) being in good agreement with previous studies (e.g., Pogge von Strandmann et al., 2019; Wilson et al., 2021).

3. Results

Background information on the soils, including physical and chemical properties and ages of the sites, was reported by Bos (2021), with selected information included in Table 1. The bulk density of the soil samples varies between 0.42 and 0.89 g/cm^3, and the pH of the pore waters exhibits a relatively narrow range between 5.8 and 6.9. The SOC values are between 2.0 % and 7.2 %, while P-Olsen values (indicating the phosphorus that can be used by plants) range from 6 to 33 μg/g. The older sites (L3, L4, and L5) have higher SOC and P-Olsen values than the younger sites (L1, L2).

The elemental and Li isotope data from the sequential leaching experiments are reported in Table 2. The four extractable fractions together represent less than 7 % of the total Li (Table 2, Fig. 2A), which is similar to results from the regolith in Hawaiian soils (Li et al., 2020), and also similar to results from leaching Icelandic river sediments (≤5%; Pogge von Strandmann et al., 2023). The Li isotope values for each fraction are shown in Fig. 2B. The exchangeable fractions have relatively high Li isotope values (mean δ^7Li = 16.2 ± 3.5 ‰, 2 s.d., n = 10), and show no clear correlations with afforestation age or sample depth. The carbonate fractions only comprise ~ 0.3 % of the total Li, with mean Li isotope values of 14.4 ± 4.4 ‰ (2 s.d., n = 10). The oxide fractions have lower Li isotope values (mean = 7.2 ± 5.7 ‰, 2 s.d., n = 10), while the clay fractions have even lower Li isotope values (mean = 2.9 ± 4.3 ‰, 2 s.d., n = 10), which are similar to the residue values that represent pristine rock (mean = 2.1 ‰, 2 s.d. = 4.4 ‰, p-value = 0.22) (Table 2).

Table 1
Basic chemical and physical data from the Icelandic soil samples. Fine-grained proportion means the weight of samples passed through 64 μm sieve / the total weight.

Sample	Fine-grained proportion	Bulk density g/cm^3	pH	SOC mg/g
L1s	0.20	0.55	6.10	35.38
L2s	0.19	0.56	6.30	27.14
L3s	0.16	0.64	6.10	45.48
L4s	0.15	0.42	5.80	71.67
L5s	0.17	0.52	5.80	59.27
L1d	0.33	0.78	6.60	32.87
L2d	0.16	0.67	6.50	46.15
L3d	0.16	0.74	6.90	52.54
L4d	0.29	0.71	6.50	63.79
L5d	0.20	0.74	6.30	35.81
HS	/	0.77	6.56	33.41
HD	/	0.89	6.60	20.10

The δ^7Li values of the exchangeable and carbonate fractions overlap with, but are generally slightly higher than, the values obtained in Hawaiian soils (10.3 to 16.4 ‰) (Li et al., 2020), while they are comparable to the exchangeable values in organic-amended basalt-rock interaction experiments (Pogge von Strandmann et al., 2022) and Icelandic river sediments (Pogge von Strandmann et al., 2023). The oxide fractions have generally lower δ^7Li values than in Hawaiian topsoils (11.1 to 17.2 ‰), but are comparable to the findings of basaltic water–rock interaction experiments (2.8 to 8.0 ‰) and Icelandic river sediments (−9.7 to 7.0 ‰) (Li et al., 2020; Pogge von Strandmann et al., 2023; Pogge von Strandmann et al., 2022). The clay fractions have slightly lower δ^7Li values than in the results of water–rock interaction experiments (5.3 to 10.8 ‰) (Pogge von Strandmann et al., 2022). As noted in Section 2, sequential leaching is not able to fully leach out the targeted fraction and it may also incorporate some contamination from other fractions, so the relative proportions of each fraction may not be fully accurate, but the differences in Li isotope composition between the fractions appear robust.

The Li isotope compositions of the plant materials are presented in Table 3. Generally, the Li isotope values of the roots and bark are low (−0.9 to 2.4 ‰, 5.6 ‰) and are comparable to those of the bulk soils (Table 2), while the leaves have the highest Li isotope values of between 5 and 22 ‰ (mean = 13 ± 12 ‰, 2 s.d., n = 5). The ground vegetation (grass) has intermediate Li isotopic compositions ranging from 0.6 to 18.6 ‰ (mean = 9.8 ‰, 2 s.d. = 12.7 ‰).

4. Discussion

4.1. Lithium isotope fractionation within plants

The Li isotope compositions of the roots (1.2 ± 2.2 ‰, 2 s.d., n = 5) are lower than those from Hawaii (~13.6 ‰) (Li et al., 2020), but higher than roots from Strengbach in France (−4.3 ‰) (Lemarchand et al., 2010). They are also slightly lower than the δ^7Li values of the bulk soils

Table 2
Elemental and Li isotope data from sequential leaching of Icelandic soils. The quantities are masses leached from 50 mg of sample (u.d.l. = under detection level). This table is also presented in https://zenodo.org/records/14194335; tab 'Sequential leaching'. The ex and carb fractions have high Na contents because of the use of Na-acetate.

Sample	Fraction	Na	Mn	Sr	Si	Al	Fe	Mg	Ca	K	Li	δ^7Li	2sd
		µg	µg	µg	µg	µg	µg	µg	µg	µg	ng	‰	
L1s	ex	22000.00	0.73	0.47	2.97	0.00	0.10	24.28	121.17	3.97	1.21	17.60	0.34
	carb	18330.00	1.49	0.30	7.68	5.02	2.96	5.67	49.68	1.97	1.06	14.33	0.09
	ox	2296.77	5.93	0.18	12.86	49.62	39.11	2.30	16.04	0.86	1.06	4.09	0.33
	cl	285.50	3.15	0.36	50.37	301.60	244.25	41.97	69.38	1.30	5.56	−1.60	0.14
	rs	682.54	104.37	9.00	/	3429.20	4888.49	1323.20	2849.81	179.86	424.95	4.39	0.57
L2s	ex	20600.00	0.21	0.21	3.03	0.00	0.20	12.70	72.38	4.43	1.09	16.22	0.39
	carb	21000.00	0.47	0.30	9.10	5.46	4.07	4.97	62.76	3.65	1.70	14.22	0.10
	ox	1972.28	5.15	0.33	11.86	67.07	46.00	1.59	19.82	1.34	1.48	7.89	0.29
	cl	280.12	5.87	0.91	295.70	425.91	267.43	16.38	64.42	1.91	3.30	3.76	0.01
	rs	572.30	96.83	7.49	/	2906.14	4574.04	1200.57	2637.04	113.81	247.29	3.06	0.25
L3s	ex	21000.00	0.20	0.41	3.13	0.00	0.27	19.62	160.53	7.25	1.05	16.87	0.06
	carb	19600.00	0.82	0.30	8.29	3.35	2.02	5.71	85.86	2.94	1.14	16.40	0.53
	ox	2229.64	2.51	0.21	14.25	42.77	16.34	3.42	34.74	1.09	0.94	9.07	0.10
	cl	240.67	2.59	0.38	63.28	261.88	199.41	28.28	87.28	2.10	3.96	1.98	0.35
	rs	434.80	81.28	4.76	/	3014.81	4844.26	747.64	1641.50	105.42	234.22	−0.75	0.44
L4s	ex	19400.00	1.29	0.36	2.37	0.00	0.45	16.40	92.33	13.04	1.09	14.15	0.00
	carb	19300.00	2.12	0.23	4.33	6.37	3.57	3.87	34.17	4.27	1.13	9.42	0.55
	ox	2466.75	2.00	0.12	4.09	33.73	17.95	0.85	10.08	1.30	0.46	0.96	0.10
	cl	284.45	7.19	0.34	80.94	455.00	233.84	11.05	69.27	1.52	3.42	2.76	0.36
	rs	870.20	86.93	7.85	/	3196.67	4053.60	1018.88	2418.03	321.66	341.59	3.21	0.15
L5s	ex	21800.00	0.26	0.20	3.50	0.00	0.73	15.39	75.95	5.71	1.17	14.92	0.50
	carb	18400.00	0.75	0.13	5.33	4.21	1.69	3.20	31.79	1.34	1.05	15.57	0.17
	ox	2880.06	2.02	0.09	10.89	39.86	19.85	1.29	14.12	0.78	0.77	8.44	0.29
	cl	488.48	4.58	0.39	65.39	308.85	275.16	57.34	144.92	3.42	7.10	2.43	0.16
	rs	681.36	88.25	7.42	/	2897.41	4298.33	1203.77	2751.48	161.98	234.04	3.26	0.04
L1d	ex	20100.00	0.15	0.54	4.51	u.d.l.	0.20	31.54	140.86	1.29	2.40	14.01	0.02
	carb	20500.00	0.29	0.31	10.03	5.29	1.90	9.18	68.14	1.15	2.24	12.62	0.34
	ox	2545.88	8.19	0.26	14.34	111.24	54.48	2.63	36.74	0.63	4.78	6.75	0.34
	cl	335.69	8.87	0.32	13.57	610.21	259.97	2.80	33.37	0.26	4.05	1.75	0.24
	rs	286.36	79.30	4.07	/	3875.64	6319.67	673.06	1503.07	49.11	203.70	−0.57	0.89
L2d	ex	22900.00	0.22	0.35	3.56	4.64	0.57	12.07	65.29	3.74	1.13	18.50	0.41
	carb	18300.00	0.33	0.55	7.69	4.80	4.91	3.84	39.38	2.45	1.10	16.92	0.41
	ox	1852.88	2.09	0.59	9.83	45.46	31.09	0.99	11.20	0.86	0.94	9.55	0.38
	cl	279.02	4.22	1.38	53.89	321.77	215.13	11.36	75.44	2.62	2.64	6.08	0.36
	rs	730.90	87.69	7.58	/	2945.25	4031.04	1100.62	2517.60	223.48	262.26	2.99	0.14
L3d	ex	21000.00	0.33	0.37	3.44	u.d.l.	0.03	28.39	148.13	0.37	1.48	19.25	0.28
	carb	18700.00	0.70	0.24	11.50	6.92	2.79	7.55	61.91	0.16	1.92	17.33	0.10
	ox	3225.81	10.97	0.18	17.23	93.40	58.01	2.67	31.02	0.39	2.80	11.79	0.34
	cl	395.47	8.63	0.25	66.45	562.49	268.36	10.30	47.03	0.66	3.22	6.39	0.44
	rs	697.47	116.74	9.67	/	3273.83	5359.96	1496.52	2957.60	140.73	279.29	5.61	0.40
L4d	ex	22700.00	0.19	0.21	3.69	u.d.l.	0.45	12.82	105.81	1.61	1.06	15.93	0.37
	carb	17100.00	0.39	0.12	6.49	1.77	2.03	3.22	33.23	0.92	0.85	13.64	0.47
	ox	4405.79	1.71	0.10	10.25	46.96	23.97	1.86	20.39	0.55	1.35	6.38	0.13
	cl	267.72	2.54	0.34	72.56	270.92	238.80	34.49	84.23	2.36	4.71	1.93	0.60
	rs	701.06	95.22	7.47	/	3012.85	4307.38	1312.85	2752.01	136.74	267.24	−0.72	0.39
L5d	ex	221200.00	0.44	0.38	4.13	u.d.l.	0.16	22.23	120.24	1.26	1.08	14.26	0.20
	carb	18900.00	0.79	0.23	9.01	6.34	3.52	4.96	61.11	0.41	1.37	13.41	0.58
	ox	2228.98	8.19	0.14	24.36	70.20	47.71	1.44	16.87	0.12	1.79	6.87	0.26
	cl	339.61	3.95	0.38	53.73	478.04	336.31	48.02	127.07	3.13	6.52	3.34	0.22
	rs	457.10	95.72	5.41	/	3386.81	5102.74	932.04	1734.68	93.39	265.91	0.61	0.44
HS	ex	18400.00	1.07	0.57	u.d.l.	u.d.l.	0.38	29.01	178.07	21.59	1.11	5.52	0.05
	carb	16000.00	4.89	0.38	u.d.l.	5.67	1.48	10.50	99.73	10.06	0.89	2.93	0.48
	ox	6687.32	15.97	0.38	18.24	72.64	19.89	6.42	85.11	5.13	1.56	−0.86	0.37
	cl	619.26	3.93	0.29	15.75	180.50	125.85	15.74	57.45	1.79	2.22	2.65	0.35
	rs	473.76	/	/	/	3631.35	5020.1	956.65	1995.87	95.87	/	2.54	0.41
HD	ex	/	/	/	/	/	/	/	/	/	/	9.95	0.27
	Carb	/	/	/	/	/	/	/	/	/	/	8.49	0.11
	Ox	/	/	/	/	/	/	/	/	/	/	5.27	0.04
	cl	/	/	/	/	/	/	/	/	/	/	3.49	0.51

(−0.8 to 5.6 ‰), the clay fraction (2.9 ± 2.2 ‰, 2 s.d., n = 5), and the oxide fraction (7.2 ± 5.7 ‰, 2 s.d., n = 5). Assuming that the exchangeable fractions (16.2 ± 3.5 ‰, 2 s.d., n = 10) have small and approximately constant offsets from the associated pore fluids ($\Delta^7Li_{(fluid-ex)}$ of 0 to 10 ‰) (Hindshaw et al., 2019), we calculate the $\Delta^7Li_{(root-fluid)}$ to be ~ −15 ‰ to −25 ‰. However, the exact source of Li to the roots in our study is unknown, as there are multiple potential Li sources in the rhizosphere, including the bulk rocks, exchangeable fractions, secondary minerals, and pore fluids (Korchagin et al., 2019; Steinhoefel et al., 2021). Regardless of the exact source, the plant roots appear to preferentially take up lighter Li isotopes than the abiotic pools. In contrast, the $\Delta^7Li_{(root-fluid)}$ values reported in the Hawaiian and Strengbach plants are small (i.e., $\delta^7Li_{(root)}$ is similar to $\delta^7Li_{(fluid)}$) (Lemarchand et al., 2010; Li et al., 2020).

The data from different organs of the plants show significantly different ranges (Table 3). The δ^7Li values of the bark are ~ 5.6 ‰ and the leaves average ~ 13.0 ‰, both significantly higher than the average values of the roots (~1.2 ‰) (Fig. 3). There is no clear relationship

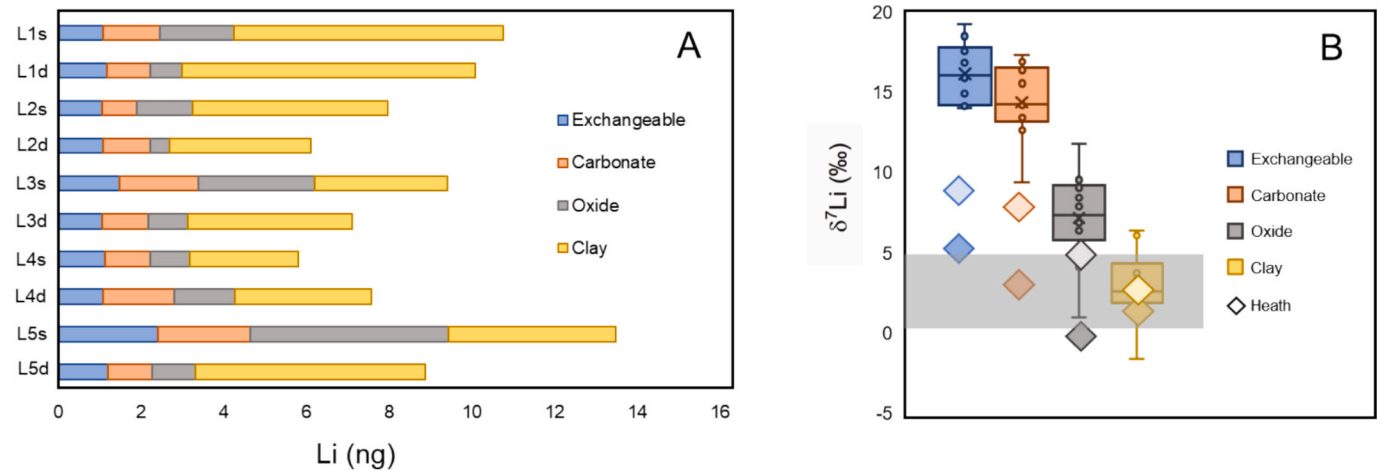

Fig. 2. Results of sequential leaching for Li. A: Amount of Li in the four extractable fractions per 50 mg sample, in the 10 afforestated soil samples. Samples L1s/d are the shallow/deep soil samples from site L1. B: Li isotope values of the extractable fractions. The small circles and box plots indicate the afforestated soil samples, while the diamonds indicate the heathland soil samples (darker diamond: HS; lighter diamond: HD). The horizontal grey bar indicates the pristine basalt Li isotope composition (Kuritani et al., 2011).

Table 3
Elemental ratios and Li isotope data from plant samples. B, bark; L, leaves; R, roots; G, ground vegetation. This table is also presented in https://zenodo.org/records/14194335; tab 'Plants'.

Sample	Li/K mg/g	Li/Na mg/g	Li/Fe mg/g	Li/Mg mg/g	Li ng/g	δ^7Li ‰	2sd
1 B	0.07	0.04	0.22	0.06	/	/	/
1 L	0.01	0.17	0.52	0.02	167	4.99	1.29
1 R	0.14	0.83	0.27	0.08	234	2.36	0.43
2 B	0.06	2.34	0.75	0.10	/	5.56	0.25
2 L	0.01	0.17	1.03	0.02	132	15.67	0.55
2 R	0.07	0.30	0.15	0.04	167	0.90	0.15
3 L	0.01	0.09	2.36	0.05	390	15.95	0.11
3 R	0.39	1.37	0.43	0.11	1216	1.70	0.06
4 L	0.01	0.00	0.79	0.03	200	21.64	0.55
4 R	0.21	0.88	0.14	0.04	533	1.68	0.94
5 L	0.00	0.02	0.49	0.02	112	6.95	0.04
5 R	0.14	0.34	0.05	0.04	481	−0.89	0.46
2 G	/	/	/	/	/	0.63	0.26
3 G	/	/	/	/	/	18.62	1.51
4 G	/	/	/	/	/	10.24	1.01
5 G	/	/	/	/	/	9.93	0.24

between the afforestation age and the Li isotope composition in each organ type, suggesting that the variation in Li isotopes is not due to ageing of the trees or the accumulation of Li from an external input with high δ^7Li values. However, there is an apparent positive correlation between the height of the plant organ (characterised by the height of the trees) and its Li isotope composition (Fig. 3A). Assuming that taller trees have longer transportation routes (e.g., roots and xylem), during which more cells could extract nutrients and other associated elements from the xylem, such a correlation could suggest that lighter Li isotopes are preferentially removed on the way to the top of the tree, with the residual heavy Li isotopes being incorporated into the leaves. In addition, such intra-plant fractionation is also seen in the leaf samples of the ground vegetation (e.g., dicots, mean = 9.8 ‰, Table 3).

The increase in Li isotope composition in the plant organs with transport is also accompanied by a decrease in Li/K and Li/Na ratios (Fig. 3B, C). These data may suggest that, during upwards transport of fluid and nutrients, Li is preferentially stored and removed compared to K and Na. The Li/K and Li/Na ratios in the leaves are between 0.001–0.15 mg/g (mean: 0.01 ± 0.008 mg/g, 2 s.d., n = 5), and 0.003–0.17 mg/g (mean: 0.09 ± 0.14 mg/g, 2 s.d., n = 5), respectively. These values are smaller than the Li/K and Li/Na ratios in the bulk rocks (1–4 mg/g and 0.34–0.7 mg/g, n = 5) and the roots (0.07–0.39 mg/g and 0.3–1.4 mg/g, n = 5), which may be taken to represent the Li released during the bio-mediated weathering processes. The preferential removal of Li during nutrient transport may be related to the toxicity of higher concentrations of Li for chlorophyll, such that plants need to prevent excess Li from entering the leaves and may do so by storing the extra Li in the vacuoles of cells that are situated at lower tree heights (e.g., root cells) (Tanveer et al., 2019). We hypothesise that, in an aggrading forest system, such excess Li might come from enhanced bio-mediated weathering of the deep regolith and/or from pore water. Specifically, the plants require sufficient nutrients (e.g., K, Mg) from rocks for growth and, considering stoichiometric release of alkaline and alkaline earth metal cations during mineral dissolution (Oelkers et al., 1994), the dissolution would provide Li that exceeds the requirements of the plants (i.e., Li/nutrient ratios in the rocks and weathering fluids would be greater than the required Li/nutrient ratios in the plants).

The above relationship between Li isotopes and proxies that potentially indicate element transport (Fig. 3B, C) agrees with the recent experimental finding that cells tend to preferentially take up ^{6}Li through Na^+/H^+ exchange (Poet et al., 2023). Lithium could migrate into the cells because it has a similar charge and/or radius to K, Mg, and Na, and plant cells could use Li to help maintain a positive internal turgor potential (force within the cell that pushes the plasma membrane against the cell wall) (Shahzad et al., 2016). Indeed, it has been shown that Li could be transported together with Na, K, and potentially Ca and Mg by the same proteins (including LCT, HKT, and NSCC) (Tanveer et al., 2019). Similar to Li isotopes, fractionation during plant transport has also been observed in other stable isotope systems, including Mg and Si isotopes (Wiggenhauser et al., 2022). We therefore suggest that the Li isotope fractionation in our samples likely arises from the following steps: 1) the presence of plants enhances the rock weathering to satisfy their need for growth and the released elements (e.g., K, Mg, Li) enter the roots; 2) the Li supply exceeds the demand of plants so excess Li is preferentially stored in cell vacuoles along the transport routes upwards; 3) when entering vacuoles, light Li is preferentially transported, while heavier Li is retained in the inter-cell fluid, and is transported upwards in transportation routes (i.e., towards leaves); 4) heavier Li reaches the leaves, where it accumulates. During this process, nutrients (e.g., K, Mg) are also transported upwards, resulting in decreasing Li/nutrient ratios. In short, the intra-plant fractionation is caused by plant cells storing excess Li (preferentially ^{6}Li) that had been obtained by the roots during rock weathering in their vacuoles.

The above observations on plant organs imply that Li could

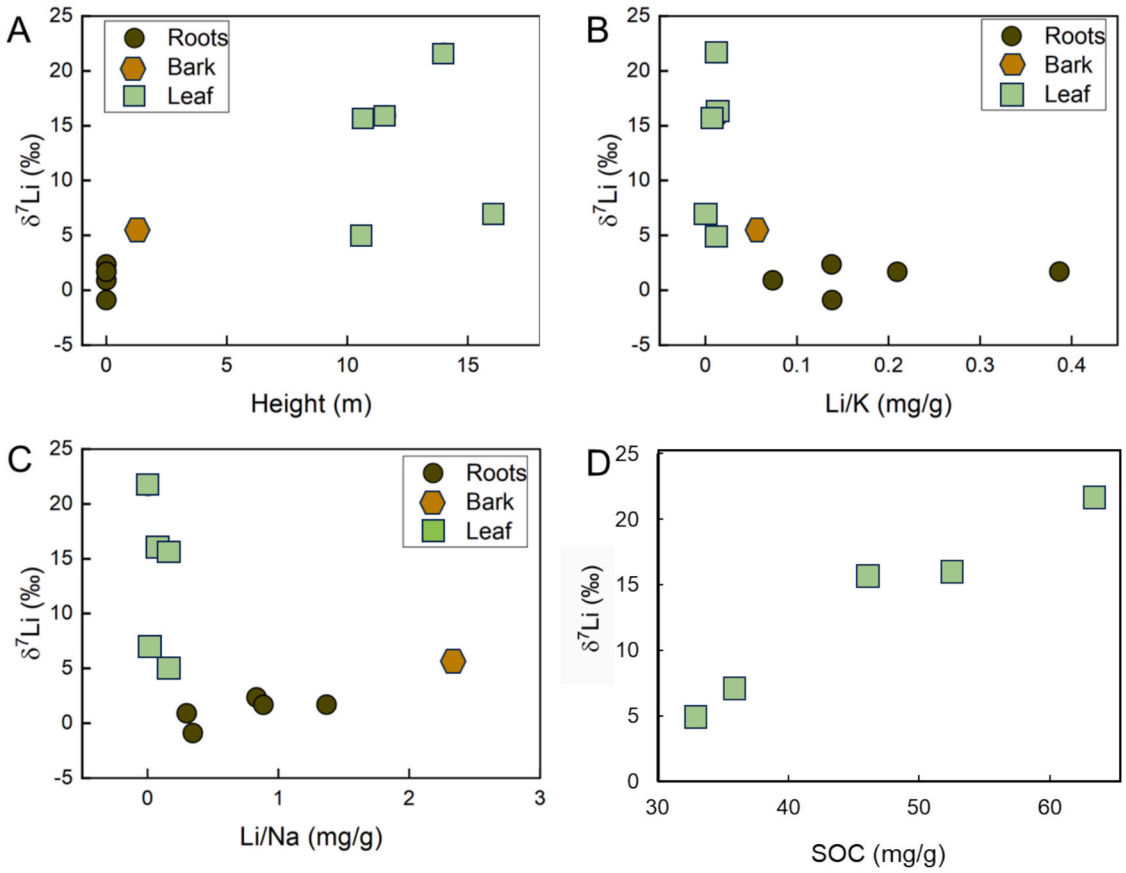

Fig. 3. Lithium isotope fractionation within plants. **A**: Li isotopes versus height of plant organs. **B**: Li isotopes versus Li/K ratios in plants. **C**: Li isotopes versus Li/Na ratios in plants. **D**: Li isotopes of leaves versus soil organic carbon (SOC) at ~ 30 cm depth.

experience isotope fractionation within plants, which may be related to the plant physiology. This finding is in contrast to previous suggestions that δ^7Li values of plants are indistinguishable from pore water or rocks (Chapela Lara et al., 2022; Clergue et al., 2015; Lemarchand et al., 2010; Steinhoefel et al., 2021). On the other hand, Li et al. (2020) suggested that light Li isotopes could be preferentially transported upwards due to kinetic isotope fractionation. The differences between our findings and those previous studies may be attributed to the growth stages of the different forests. In our case, the forests are still under their initial aggrading stage, such that excess Li (together with other necessary nutrient elements) could be supplied by bio-mediated weathering into the plants. In contrast, the previous studies investigated forests approaching the end of their aggrading stage or in steady-state (Chapela Lara et al., 2022; Clergue et al., 2015; Lemarchand et al., 2010). Steady-state forests tend to recycle nutrients from the topsoils instead of weathering fresh rocks (Balogh-Brunstad et al., 2008), which could prevent excess amounts of Li being released from rock weathering and entering into the root cells, potentially decreasing the potential for Li isotope fractionation within plants. This finding is also supported by the positive correlation between SOC content (especially in deeper topsoils at ~ 30 cm) and δ^7Li values of the leaves (Fig. 3D). If we assume that a higher SOC content suggests that less decomposition of organic matter is occurring, we might infer less elemental recycling of nutrients from organic compounds, such that there is more use of root exudates (i.e., organic acids) to enhance mineral dissolution to obtain nutrients from the soil. However, we caution that this scenario is just one possibility to explain the differences in the observations between the above studies, and more work on the behaviour of Li isotopes in forest ecosystems is needed to fully understand the processes involved.

4.2. The influence of afforestation on Li isotopes in the extractable fraction of soils

Sequential leaching was applied to target the extractable fractions (exchangeable, carbonate, oxide, and clay) in soils. These fractions could have formed rapidly, with the exchangeable fraction reaching equilibrium on a timescale of days (e.g., Zhang et al., 2021), and they represent a small part of the bulk soil (< 7 % in total), allowing them to respond sensitively to weathering processes (e.g., Pogge von Strandmann et al., 2019). However, phases other than the targeted fraction could also be leached, making it necessary to assess the validity of the measurements (Pogge von Strandmann et al., 2019).

For the exchangeable and carbonate fractions, contamination from Al/Si-bearing minerals should be avoided (Pogge von Strandmann et al., 2023). The exchangeable and carbonate fractions in our samples have low Al/Ca ratios (e.g., Al is below the detection limit in the exchangeable fraction), which rules out a significant influence of contamination from the silicate or oxide fractions. The exchangeable and carbonate fractions from the afforested soils have higher Li isotope compositions (mean values of 16.2 and 14.4 ‰, respectively) than in the heathland soils (ex: 9.9 and 5.5 ‰, carb: 8.4 and 2.9 ‰) (Fig. 2B).

The oxide fractions have high Al/Si ratios (2.8 to 8.2 mol/mol) and low Fe/Al ratios (0.38 to 0.78 mol/mol), and the Li content is proportional to the Al content in this fraction (Fig. 4A). Considering that oxide minerals contain negligible Si, and that pristine basalt rocks have Al/Si ratios ~ 0.25 mol/mol (Kuritani et al., 2011), these higher ratios may suggest that this fraction is dominated by the extraction of Al-bearing secondary minerals (i.e., not basalt residue), such as allophane (Al/Si = 2), gibbsite ($Al(OH)_3$), or other amorphous Al-bearing minerals (Pogge von Strandmann et al., 2021b). On the other hand, the Li content in the clay fraction is weakly related to the Fe content in the clay fraction

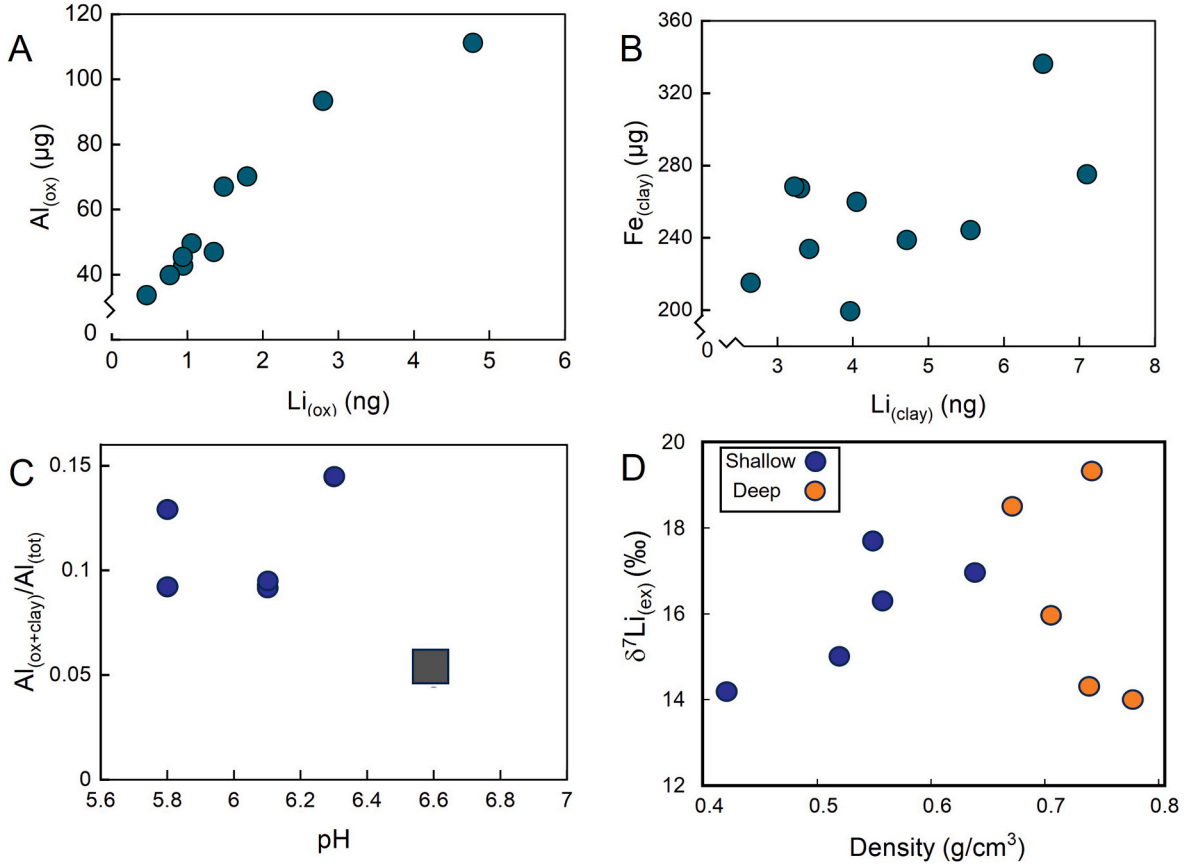

Fig. 4. Controlling factors on the extractable fractions. **A**: Li content in the oxide fraction correlates with the Al content in this fraction (values plotted are the amounts leached from 50 mg of soil). **B**: Li content in the clay fraction correlates weakly with the Fe content in this fraction (values plotted are the amounts leached from 50 mg of soil). **C**: $Al_{(oxide+clay)}/Al_{(total)}$ in shallow soil sample vs. soil pH values (the grey square indicates the HS sample). **D**: Li isotopes in the exchangeable fraction do not correlate with bulk soil density.

(Fig. 4B), potentially indicating that this fraction is dominated by Fe-bearing secondary minerals. Also, as the Al/Si (1.4 to 8.9 mol/mol) and Fe/Si (0.9 to 19.1 mol/mol) ratios in the clay fraction are significantly higher than in the pristine basalt (~0.25 mol/mol, ~0.2 mol/mol, respectively) (Kuritani et al., 2011), this fraction is evidently not dominated by pristine basalt residues. Since both fractions appear to have extracted predominantly Al- and/or Fe- bearing secondary minerals, we consider that the sum of the oxide and clay fractions could be used to represent the combined secondary mineral fraction in the soil samples. The average Li isotope compositions of the oxide fractions in the afforested soil samples (7.2 ‰) are higher than those from the heathland soil (5.3 ‰ and -0.86 ‰) (Fig. 2B), while those of the clay fractions are similar (mean of afforestated soil sample: 2.9 ‰, to 2.7 ‰ and 3.5 ‰ in heathland soil) (Fig. 2B).

The elevated Li isotope compositions in the extractable fractions of the afforested soil samples cannot be explained by the geochemical variability of the substrate or by atmospheric inputs such as volcanic ash, because the samples were collected from adjacent soil plots (Fig. 1). In addition, a simple calculation, assuming that the rain Li concentration is 6 ng/L (Vigier et al., 2009), suggests that rainfall could only provide 0.4 ng/m^2/yr of Li to the topsoil. In comparison, a 1 m^2 area of the top 10 cm of the soil contains a total Li reservoir of 330 mg (based on a density of ~ 550 kg/m^3 and an average Li concentration of ~ 6 μg/g) (Pogge von Strandmann et al., 2021a), indicating that rainfall inputs are an insignificant contributor to the Li budget. Due to their spatial proximity, with the heathland plot less than 1 km away from plots L1 and L4 and situated on the same stream, inheriting Li isotope signals from upstream fluids with significantly diverging Li isotope signatures is also unlikely (Pogge von Strandmann et al., 2021a).

However, such differences in Li isotope composition of the extractable fractions might be explained by several aspects of the afforestation processes. One potential mechanism is the addition of leaves with heavy Li isotope compositions onto the topsoils. Lithium isotopes are highly fractionated within plants (Section 4.1), so when the leaves with high δ^7Li values fall back to the topsoils (i.e., 0–10 cm) annually and are decomposed by micro-organisms, they would elevate the δ^7Li values of the pore fluid. These elevated Li isotope signatures could then be inherited by the extractable fractions in soils, and be uptaken by roots, subsequently helping to produce leaves with heavier Li isotope compositions. In support of this mechanism, the addition of litterfall has previously been reported in these plots, with soils from 0-10 cm depth having more than 3 times higher SOC levels than the deeper soils (Bos, 2021). In addition, the recycling of Li has been demonstrated in Hawaiian soils (Li et al., 2020), and similar recycling mechanisms were found in other metal isotope systems (Bolou-Bi et al., 2012; Kimmig et al., 2018; Opfergelt et al., 2017).

We further tested this litterfall hypothesis using mass balance calculations. Given that Siberian larch is deciduous, we obtain the total litterfall addition by estimating the total biomass of leaves from the size of the trees (Bjarnadóttir et al., 2007). Assuming the diameter (D) of the trees is 10 cm, we calculate the total biomass of leaves = 17.8 * $D^{1.81}$ = 1.15 kg for one tree. The mean density of standing stems is taken as 2500/ha, equivalent to 0.25 trees/m^2. Therefore, the biomass addition from leaves is ~ 0.29 kg/m^2/yr, which is similar to estimates from forests in Strengbach (0.3 kg/m^2/yr) (Lemarchand et al., 2010). With a Li concentration of ~ 200 ng/g (Table 2), the annual addition of Li to the forest floor is ~ 58 μg/m^2/yr. In comparison, a 1 m^2 area of the top 10 cm of the soil contains a total Li reservoir of 330 mg. Of this reservoir,

the exchangeable and carbonate fractions make up ~ 1 % (i.e., 3.3 mg), while the secondary mineral fraction makes up ~ 2 % (i.e., 6.6 mg). Hence, the combined exchangeable and carbonate reservoir alone would require ~ 60 years for litterfall to fully replenish it, which is comparable to the longest afforestation age (63 years) in this study. However, if we consider that the litterfall was likely not completely decomposed, and that Li was also partially lost to the fluids and potentially removed from the catchments, then the decomposition of litterfall probably cannot be the sole mechanism responsible for increasing the Li isotope values in these fractions.

In a second potential mechanism, the afforestation process could also change the chemistry and Li isotope composition of the extractable fractions indirectly, by influencing the formation of secondary minerals. This process is demonstrated by the increase in the $Al_{(oxide+clay)}/Al_{(total)}$ ratio (a proxy potentially indicating the proportion of secondary minerals in soils) between the heathland soil samples and the afforested soil samples (Fig. 4C). According to transition state theory, secondary mineral formation is determined by factors including the saturation state of the fluids (dependent on ion activity, pH, reactive surface and cation concentrations), the presence of nucleation sites, temperature, and mineralogy (Lasaga, 1984). In this case, afforestation could influence secondary mineral formation via both chemical and physical processes. Here we outline two possible scenarios, before testing them below. One chemically-driven scenario involves enhancement of the weathering rate, which could arise from a lowering of the pH values in the afforested soils due to organic carbon decomposition (Bos, 2021) and/or root growth (i.e., increasing reactive surface), and which would in turn provide more metal cations and enhanced alkalinity for secondary mineral formation. A second physically-driven scenario is related to increasing local particle and water residence times, which could arise from the effects of a closed canopy (decreasing rainfall impact and evaporation), root stabilisation, or changing soil structure (Brantley et al., 2017), and which would also favour the formation of secondary minerals.

In the chemically-driven scenario, an increase in the secondary mineral content could be related to an increase in the weathering rate via changing mineral reactive surface (e.g., root separation) or changes in soil fluid chemistry (e.g., pH). Assuming that taller trees have deeper roots, the plots with the tallest trees (L5) have $Al_{(oxide+clay)}/Al_{(total)}$ ratios of 0.09 (shallow soil) and 0.13 (deep soil), which are intermediate among the 10 afforested samples (Table 1, 2), suggesting that such an increase might not be directly related to the growth of deeper roots. In contrast, the $Al_{(oxide+clay)}/Al_{(total)}$ ratio in the shallow heathland soil samples (~0.06) is half of that in the shallow afforested soils (mean ~0.11), indicating more restricted secondary mineral formation (Fig. 4C). Such differences in the ratio may be related to soil pH values: the shallow afforestated topsoils (10 cm) have lower pH values, in which lower pH conditions increase rock dissolution and promote the formation of more Al-bearing secondary minerals (including amorphous minerals) (Mulders and Oelkers, 2021) (Fig. 4C). In turn, a greater content of secondary minerals in afforested samples would provide more reactive sites for Li incorporation and/or adsorption, enabling more fractionation of Li isotopes in the pore fluids (Pogge von Strandmann et al., 2021a), and could explain the low δ^7Li values in the secondary minerals from the heathland site ($\delta^7Li_{(ox)}$ = -0.8 ‰ and 5.3 ‰).

The specific origin of the pH decrease is unknown, although the lower pH of the shallow topsoils than the deeper topsoils could indicate a link to the litterfall decomposition (Bos, 2021). Alternatively, or in addition, the possibility of root respiration or root exudates driving this change cannot be excluded. As water infiltrates through the afforested soil column from above, the Li added from litterfall decomposition ($\delta^7Li \approx 13$ ‰) and from primary mineral dissolution ($\delta^7Li \approx 0$ to 5 ‰) could be incorporated into secondary mineral fractions in the shallow topsoils ($\delta^7Li_{(ox)} = 6.1$ ‰, $\delta^7Li_{(cl)} = 1.8$ ‰), leaving fluid with more fractionated Li isotope compositions to continue downwards, thereby increasing the δ^7Li values of the secondary mineral fractions in the deeper topsoils ($\delta^7Li_{(ox)} = 8.3$ ‰, $\delta^7Li_{(cl)} = 3.8$ ‰). As reported in previous studies, Li isotope compositions of soils in non-forested sites in Iceland were significantly controlled by rapidly-forming amorphous Al-bearing secondary minerals (e.g., allophane) (Pogge von Strandmann et al., 2021a), indicating that the formation of secondary minerals could change the Li isotope compositions in the extractable fractions over decadal timescales, as also observed here.

Afforestation may also enhance secondary mineral formation through physical mechanisms, particularly by influencing the water residence time (Pogge von Strandmann et al., 2023; Wilson et al., 2021; Zhang et al., 2022). Natural processes such as bioturbation, root stabilisation, and canopy closure, as well as human processes such as tree thinning operations, could all influence this parameter. However, if we assume that a higher soil bulk density indicates a lower porosity and a higher organic matter content (Bos, 2021), which would likely translate to a longer water residence time, the lack of correlation between soil bulk density and $\delta^7Li_{(ex)}$ values (Fig. 4D) suggests that differences in water residence time may not be a dominant controlling factor in this setting. We therefore suggest that the integrated mechanisms of litterfall addition and chemically-driven secondary mineral formation are likely to be the main controls on the Li isotope compositions in the extractable fractions of the afforested soils in our study, similar to results from Hawaiian soils (Li et al., 2020). In addition to the influences from litter recycling and secondary mineral formation, a decrease in surface soil erosion linked to afforestation could also have helped the afforested topsoils to preserve these features (Johnson, 1990).

Additional direct and/or indirect mechanisms can also be envisaged to arise from afforestation, but they are difficult to simultaneously assess using Li isotopes. For example, the presence of organic compounds could affect element complexation in soil pore waters and the secondary mineral nucleation and growth (Tazaki, 2005). However, the existing measurements and understanding are not sufficient to assess the role of organic compounds because the species of organic compounds present in the soil pore waters are unknown.

4.3. Time dependency of Li isotopes following afforestation

This study also aimed to investigate the temporal evolution of Li isotopes in soils following afforestation. Based on the data from the chronosequences, the Li isotopes in the exchangeable fractions decrease slightly with age by ~ 3 ‰ from the shallow soils of L1 to L5, but these changes are much smaller than the total changes due to afforestation (increases of ~ 10 ‰) (Fig. 5). Meanwhile, the Li isotopes in the carbonate, oxide, and clay fractions show no clear temporal trends from L1 to L5. In the extracted fractions of the deeper soils, a 'hump-back shape' curve is observed for Li isotopes through time, with peak values in the samples from 31-32 years and a variation range of ~ 5 ‰ (Fig. 5B). This temporal evolution may indicate that the influence of afforestation on weathering reached a peak within less than ~ 40 years in these samples. In addition, all the fractions show a similar temporal trend (Fig. 5B), suggesting that the four fractions of the deeper soils may be at least partly controlled by the same set of mechanisms. However, since these findings are based on only five time slices, which were unequally spaced through time, more detailed studies will be required to confirm and further explore these trends. In particular, any trends within the first couple of decades of afforestation were not accessible within our study and this time interval should be explored in future.

The above temporal variations in Li isotopes in the extractable fractions may arise from a combination of at least four different (but potentially inter-related) controls: (i) water residence time that is mainly determined by changes in the thickness and physical properties of soil (Pogge von Strandmann et al., 2023; Wilson et al., 2021), (ii) changes in secondary mineralogy (Pistiner and Henderson, 2003) or the maturation of secondary minerals, (iii) changes in fluid chemistry driven by mineral dissolution, variable secondary mineral formation (potentially linked to plant physiology and ecosystem development), and the

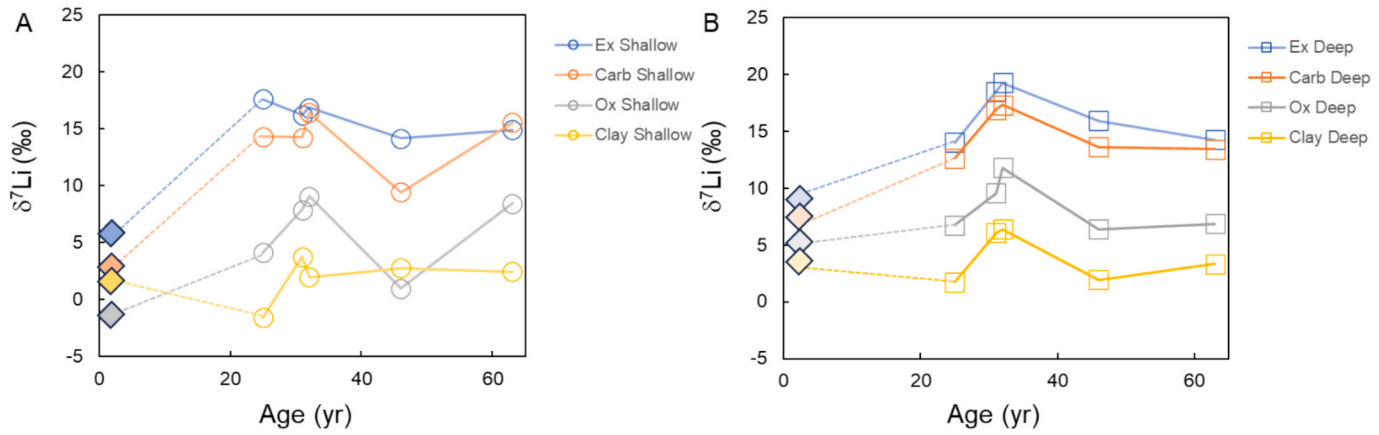

Fig. 5. Evolution of Li isotope composition with time in each extractable fraction. **A**: Evolution in shallow soils. **B**: Evolution in deep soils. The diamonds represent the Li isotope compositions of the extractable fractions in the heathland samples.

physical properties of soils, and (iv) variations due to litterfall addition (potentially also linked to plant physiology). However, these mechanisms are interconnected and are hard to deconvolve with our current understanding and measurements.

4.4. Implications

The Li isotope increase of ~ 10 ‰ in the extractable fractions of the soils following afforestation occurred rapidly (<25 years) (Fig. 5) in comparison to the growth timescales of trees (>100 years). Given that the extractable fractions largely represent the secondary mineral products of weathering processes, this finding suggests that the influence of afforestation on the chemical weathering of silicate rocks is rapid, and may even be considered as instantaneous when considering geological timescales (>1 kyr). Hence, the changing presence of vascular plants on Earth's surface could be expected to rapidly affect weathering processes, the rate of secondary mineral formation, and the Li isotope composition of the critical zone and the oceans, as recently proposed (Kalderon-Asael et al., 2021). We therefore emphasise that studies applying Li isotopes to understand the evolution of the critical zone, or for paleoenvironmental reconstructions more broadly, should carefully consider the influences from the waxing and waning of forest ecosystems (e.g., Zhang et al., 2023).

The observed variations of Li isotope fractionation between different plant organs suggest that, similar to other elements, Li isotopes could be fractionated during biological processes. Furthermore, the recycling of leaf litter in topsoils could influence the Li isotope budget of soils, particularly during the aggrading stage of forest growth. As such, there are both direct and indirect mechanisms through which plants, as a part of forest ecosystems, may influence Li isotopes in soils and the surficial environment. Once forest ecosystems are approaching steady-state, the higher nutrient recycling rates could lead to less rock weathering by the roots, and reduced potential for Li isotope fractionation within plants. Therefore, estimates of bio-mediated weathering rates, whether made using Li isotopes or other approaches, may be dependent on the growth stage of plants (Balogh-Brunstad et al., 2008), and estimates from experiments or observations from single-point sampling should be applied to longer timescales (e.g., >1 kyr) with caution.

5. Conclusions

To understand the behaviour of plant-mediated silicate weathering in afforested soils, we measured Li isotopes on plant organs, and in sequential leachates from soil chronosequence samples spanning 25 to 63 years after afforestation and two heathland control samples. The results from plant organs show that Li isotopes can be fractionated within plants, with significantly heavier Li isotope signatures in the leaves than the roots. We suggest that this fractionation might arise from plants storing the excess light Li in vacuoles, and thereby restricting the Li transport into leaves where photosynthesis occurs. The extractable fractions (exchangeable, carbonate, oxide fractions) of the afforested soils have δ^7Li values that are ~ 10 ‰ higher than those of heathland soils. Such a change is attributed to the integrated effects of both litterfall decomposition and afforestation-mediated secondary mineral formation. This finding indicates that afforestation could significantly influence both Li isotope compositions and silicate weathering over short timescales (<25 years), and highlights the potential importance of terrestrial forest evolution as a driver of Li isotope changes in both the critical zone and seawater over Earth's Phanerozoic history.

CRediT authorship contribution statement

Xianyi Liu: Writing – review & editing, Writing – original draft, Visualization, Methodology, Investigation, Formal analysis, Data curation, Conceptualization. **David J. Wilson:** Writing – review & editing, Supervision, Investigation, Conceptualization. **Kevin W. Burton:** Writing – review & editing, Resources, Conceptualization. **Bjarni Diðrik Sigurdsson:** Writing – review & editing, Resources. **Julia C. Bos:** Writing – review & editing, Resources. **Wesley T. Fraser:** Writing – review & editing, Investigation. **Philip A.E. Pogge von Strandmann:** Writing – review & editing, Supervision, Investigation, Funding acquisition, Conceptualization.

Declaration of competing interest

The authors declare that they have no known competing financial interests or personal relationships that could have appeared to influence the work reported in this paper.

Acknowledgements

P.P.v.S. is supported by ERC grant 682760 CONTROLPASTCO2, which also supported analyses. D.J.W. is supported by a Natural Environment Research Council independent research fellowship (NE/T011440/1). We thank Gary Tarbuck for assistance with the concentration and isotope measurements, Dr Chunyao Liu for help with the Li isotope purification process, and Dr Xu (Yvon) Zhang, Dr Hugo de Boer, Dr Boris Jansen and Dr Nan Zhang for their constructive advice. For the purpose of open access, the author has applied a 'Creative Commons Attribution (CC BY) licence' to any Author Accepted Manuscript version arising.

Data availability

Data for Rapid and significant lithium isotope response to afforestation in Icelandic topsoils (Original data) ((Zenodo))

References

Arnalds, Ó., Hallmark, C., Wilding, L., 1995. Andisols from four different regions of Iceland. Soil Sci. Soc. Am. J. 59, 161–169.

Balogh-Brunstad, Z. et al., 2008. Chemical weathering and chemical denudation dynamics through ecosystem development and disturbance. Global Biogeochemical Cycles, 22.

Berner, E.K., Berner, R.A., Moulton, K.L., 2003. 5.06 - Plants and Mineral Weathering: Present and Past. In: Holland, H.D., Turekian, K.K. (Eds.), Treatise on Geochemistry. Pergamon, Oxford, pp. 169–188.

Bjarnadóttir, B., Inghammar, A.C., Brinker, M.-M., Sigurdsson, B.D., 2007. Single tree biomass and volume functions for young Siberian larch trees (Larix sibirica) in eastern Iceland. Icel. Agric. Sci. 20, 125–135.

Bolou-Bi, E.B., Vigier, N., Poszwa, A., Boudot, J.-P., Dambrine, E., 2012. Effects of biogeochemical processes on magnesium isotope variations in a forested catchment in the Vosges Mountains (France). Geochim. Cosmochim. Acta 87, 341–355.

Bonneville, S., et al., 2011. Tree-mycorrhiza symbiosis accelerate mineral weathering: Evidences from nanometer-scale elemental fluxes at the hypha–mineral interface. Geochim. Cosmochim. Acta 75, 6988–7005.

Bos, J.C., 2021. Effects of afforestation on soil properties, ecosystem carbon stocks and biodiversity in East Iceland. Agricultural University of Iceland (m.sc. Thesis).

Brantley, S.L., et al., 2017. Reviews and syntheses: on the roles trees play in building and plumbing the critical zone. Biogeosciences 14.

Cai, D., Henehan, M.J., Uhlig, D., von Blanckenburg, F., 2024. Lithium isotopes in water and regolith in a deep weathering profile reveal imbalances in Critical Zone fluxes. Geochim. Cosmochim. Acta 369, 213–226.

Campbell, J.S., et al., 2022. Geochemical negative emissions technologies: Part I. Review.

Chapela Lara, M., Buss, H.L., Henehan, M.J., Schuessler, J.A., McDowell, W.H., 2022. Secondary Minerals Drive Extreme Lithium Isotope Fractionation During Tropical Weathering. J. Geophys. Res. Earth 127, e2021JF006366.

Clergue, C., et al., 2015. Influence of atmospheric deposits and secondary minerals on Li isotopes budget in a highly weathered catchment, Guadeloupe (Lesser Antilles). Chem. Geol. 414, 28–41.

Dakora, F.D., Phillips, D.A., 2002. Root exudates as mediators of mineral acquisition in low-nutrient environments, Food security in nutrient-stressed environments: Exploiting plants' genetic capabilities. Springer 201–213.

Dontsova, K., Balogh-Brunstad, Z., Chorover, J., 2020. Plants as Drivers of Rock Weathering. Ecological Drivers and Environmental Impact, Biogeochemical Cycles, pp. 33–58.

Edwards, D.P., et al., 2017. Climate change mitigation: potential benefits and pitfalls of enhanced rock weathering in tropical agriculture. Biol. Lett. 13, 20160715.

Gou, L.-F., Liu, C.-Y., Deng, L., Jin, Z., 2020. Quantifying the impact of recovery during chromatographic purification on the accuracy of lithium isotopic determination by multi-collector inductively coupled plasma mass spectrometry. Rapid Commun. Mass Spectrom. 34, e8577.

Hathorne, E.C., James, R.H., 2006. Temporal record of lithium in seawater: A tracer for silicate weathering? Earth Planet. Sci. Lett. 246, 393–406.

Hindshaw, R.S., et al., 2019. Experimental constraints on Li isotope fractionation during clay formation. Geochim. Cosmochim. Acta 250, 219–237.

Johnson, D.L., 1990. Biomantle evolution and the redistribution of earth materials and artifacts. Soil Sci. 149, 84–102.

Jones, D.L., 1998. Organic acids in the rhizosphere – a critical review. Plant and Soil 205, 25–44.

Kalderon-Asael, B., et al., 2021. A lithium-isotope perspective on the evolution of carbon and silicon cycles. Nature 595, 394–398.

Kantola, I.B., Masters, M.D., Beerling, D.J., Long, S.P., DeLucia, E.H., 2017. Potential of global croplands and bioenergy crops for climate change mitigation through deployment for enhanced weathering. Biol. Lett. 13, 20160714.

Kimmig, S.R., Holmden, C., Bélanger, N., 2018. Biogeochemical cycling of Mg and its isotopes in a sugar maple forest in Québec. Geochim. Cosmochim. Acta 230, 60–82.

Korchagin, J., Bortoluzzi, E.C., Moterle, D.F., Petry, C., Caner, L., 2019. Evidences of soil geochemistry and mineralogy changes caused by eucalyptus rhizosphere. Catena 175, 132–143.

Kulmatiski, A., Beard, K.H., Stevens, J.R., Cobbold, S.M., 2008. Plant–soil feedbacks: a meta-analytical review. Ecol. Lett. 11, 980–992.

Kuritani, T., Yokoyama, T., Kitagawa, H., Kobayashi, K., Nakamura, E., 2011. Geochemical evolution of historical lavas from Askja Volcano, Iceland: Implications for mechanisms and timescales of magmatic differentiation. Geochim. Cosmochim. Acta 75, 570–587.

Lasaga, A.C., 1984. Chemical kinetics of water-rock interactions. J. Geophys. Res. Solid Earth 89 (B6), 4009–4025.

Lemarchand, E., Chabaux, F., Vigier, N., Millot, R., Pierret, M.-C., 2010. Lithium isotope systematics in a forested granitic catchment (Strengbach, Vosges Mountains, France). Geochim. Cosmochim. Acta 74, 4612–4628.

Lenton, T.M., Crouch, M., Johnson, M., Pires, N., Dolan, L., 2012. First plants cooled the Ordovician. Nat. Geosci. 5, 86–89.

Li, W., Liu, X.-M., 2020. Experimental investigation of lithium isotope fractionation during kaolinite adsorption: Implications for chemical weathering. Geochim. Cosmochim. Acta 284, 156–172.

Li, W., Liu, X.-M., Chadwick, O.A., 2020. Lithium isotope behavior in Hawaiian regoliths: Soil-atmosphere-biosphere exchanges. Geochim. Cosmochim. Acta 285, 175–192.

Liu, C.Y., Pogge von Strandmann, P.A., Tarbuck, G., Wilson, D.J., 2022. Experimental Investigation of Oxide Leaching Methods for Li Isotopes. Geostand. Geoanal. Res.

Lucas, Y., 2001. The Role of Plants in Controlling Rates and Products of Weathering: Importance of Biological Pumping. Annu. Rev. Earth Planet. Sci. 29, 135–163.

Misra, S., Froelich, P.N., 2012. Lithium Isotope History of Cenozoic Seawater: Changes in Silicate Weathering and Reverse Weathering. Science 335, 818–823.

Mulders, J.J.P.A., Oelkers, E.H., 2021. An experimental study of sepiolite dissolution and growth rates as function of the aqueous solution saturation state at 60 °C. Geochim. Cosmochim. Acta 315, 276–294.

Oelkers, E.H., Schott, J., Devidal, J.-L., 1994. The effect of aluminum, pH, and chemical affinity on the rates of aluminosilicate dissolution reactions. Geochim. Cosmochim. Acta 58, 2011–2024.

Oeser, R.A., von Blanckenburg, F., 2020. Do degree and rate of silicate weathering depend on plant productivity? Biogeosciences 17, 4883–4917.

Opfergelt, S., et al., 2017. The influence of weathering and soil organic matter on Zn isotopes in soils. Chem. Geol. 466, 140–148.

Penniston-Dorland, S., Liu, X.-M., Rudnick, R.L., 2017. Lithium Isotope Geochemistry. Rev. Mineral. Geochem. 82, 165–217.

Pistiner, J.S., Henderson, G.M., 2003. Lithium-isotope fractionation during continental weathering processes. Earth Planet. Sci. Lett. 214, 327–339.

Poet, M., et al., 2023. Biological Fractionation of Lithium Isotopes by Cellular Na+/h+ Exchangers Unravels Fundamental Transport Mechanisms. iScience, 26, 106887.

Pogge von Strandmann, P.A., et al., 2021a. The lithium isotope response to the variable weathering of soils in Iceland. Geochim. Cosmochim. Acta 313, 55–73.

Pogge von Strandmann, P.A. et al., 2021b. Lithium isotope evidence for enhanced weathering and erosion during the Paleocene-Eocene Thermal Maximum. Science advances, 7, eabh4224.

Pogge von Strandmann, P.A.E., et al., 2023. Assessing hydrological controls on the lithium isotope weathering tracer. Chem. Geol. 642, 121801.

Pogge von Strandmann, P.A.E., Dellinger, M., West, A.J., 2021b. Lithium Isotopes: A Tracer of Past and Present Silicate Weathering. Cambridge University Press, Cambridge.

Pogge von Strandmann, P.A.E., et al., 2019. Experimental determination of Li isotope behaviour during basalt weathering. Chem. Geol. 517, 34–43.

Pogge von Strandmann, P.A.E., Jenkyns, H.C., Woodfine, R.G., 2013. Lithium isotope evidence for enhanced weathering during Oceanic Anoxic Event 2. Nat. Geosci. 6, 668–672.

Pogge von Strandmann, P.A.E., et al., 2022. Lithium isotope behaviour during basalt weathering experiments amended with organic acids. Geochim. Cosmochim. Acta 328, 37–57.

Pogge von Strandmann, P.A.E., et al., 2014. Chemical weathering processes in the Great Artesian Basin: Evidence from lithium and silicon isotopes. Earth Planet. Sci. Lett. 406, 24–36.

Ritter, E., 2007. Carbon, nitrogen and phosphorus in volcanic soils following afforestation with native birch (Betula pubescens) and introduced larch (Larix sibirica) in Iceland. Plant and Soil 295, 239–251.

Ritter, E., 2009. Development of bioavailable pools of base cations and P after afforestation of volcanic soils in Iceland. For. Ecol. Manage. 257, 1129–1135.

Rosenstock, N.P., van Hees, P.A.W., Fransson, P.M.A., Finlay, R.D., Rosling, A., 2019. Biological enhancement of mineral weathering by Pinus sylvestris seedlings – effects of plants, ectomycorrhizal fungi, and elevated CO2. Biogeosciences 16, 3637–3649.

Rudnick, R.L., Tomascak, P.B., Njo, H.B., Gardner, L.R., 2004. Extreme lithium isotopic fractionation during continental weathering revealed in saprolites from South Carolina. Chem. Geol. 212, 45–57.

Shahzad, B., et al., 2016. Lithium toxicity in plants: Reasons, mechanisms and remediation possibilities – A review. Plant Physiol. Biochem. 107, 104–115.

Sigurdsson, B.D., Magnusson, B., Elmarsdottir, A., Bjarnadottir, B., 2005. Biomass and composition of understory vegetation and the forest floor carbon stock across Siberian larch and mountain birch chronosequences in Iceland. Ann. For. Sci. 62, 881–888.

Steinhoefel, G., Brantley, S.L., Fantle, M.S., 2021. Lithium isotopic fractionation during weathering and erosion of shale. Geochim. Cosmochim. Acta 295, 155–177.

Tanveer, M., Hasanuzzaman, M., Wang, L., 2019. Lithium in environment and potential targets to reduce lithium toxicity in plants. J. Plant Growth Regul. 38, 1574–1586.

Tazaki, K., 2005. Microbial formation of a halloysite-like mineral. Clay Clay Miner. 53, 224–233.

Uhlig, D., Schuessler, J.A., Bouchez, J., Dixon, J.L., von Blanckenburg, F., 2017. Quantifying nutrient uptake as driver of rock weathering in forest ecosystems by magnesium stable isotopes. Biogeosciences 14, 3111–3128.

Vigier, N., Gislason, S.R., Burton, K.W., et al., 2009. The relationship between riverine lithium isotope composition and silicate weathering rates in Iceland. Earth Planet. Sci. Lett. 287 (3–4), 434–441.

Walker, J.C.G., Hays, P.B., Kasting, J.F., 1981. A negative feedback mechanism for the long-term stabilization of Earth's surface temperature. J. Geophys. Res. Oceans 86, 9776–9782.

West, A.J., Galy, A., Bickle, M., 2005. Tectonic and climatic controls on silicate weathering. Earth Planet. Sci. Lett. 235, 211–228.

Wiggenhauser, M., et al., 2022. Stable isotope fractionation of metals and metalloids in plants: A review. Front. Plant Sci. 13.

Wilson, D.J., et al., 2021. Seasonal variability in silicate weathering signatures recorded by Li isotopes in cave drip-waters. Geochim. Cosmochim. Acta 312, 194–216.

Zhang, F., et al., 2022. Hydrological control of river and seawater lithium isotopes. Nat. Commun. 13, 3359.
Zhang, X., et al., 2023. Evolution of the alpine Critical Zone since the Last Glacial Period using Li isotopes from lake sediments. Earth Planet. Sci. Lett. 624, 118463.
Zhang, X., et al., 2021. Experimental constraints on Li isotope fractionation during the interaction between kaolinite and seawater. Geochim. Cosmochim. Acta 292, 333–347.